ACS APPLIED MATERIALS & INTERFACES

Research Article

www.acsami.org

In Situ Magnetic Field-Assisted Low Temperature Atmospheric Growth of GaN Nanowires via the Vapor−Liquid−Solid Mechanism

Jun Sik Kim,[∥,†,‡] Bhaskar Chandra Mohanty,[∥,†,⊥] Chan Su Han,[†] Seung Jun Han,[‡] Gwang Heon Ha,[‡] Liwei Lin,[§] and Yong Soo Cho*[,†]

[†]Department of Materials Science & Engineering, Yonsei University, Seoul 120-749, Korea

[‡]R&D Center, LG Displays Co. Ltd., Paju-si, Gyeonggi-do 413-811, Korea

[§]Department of Mechanical Engineering, University of California at Berkeley, Berkeley, California 94720-1740, United States

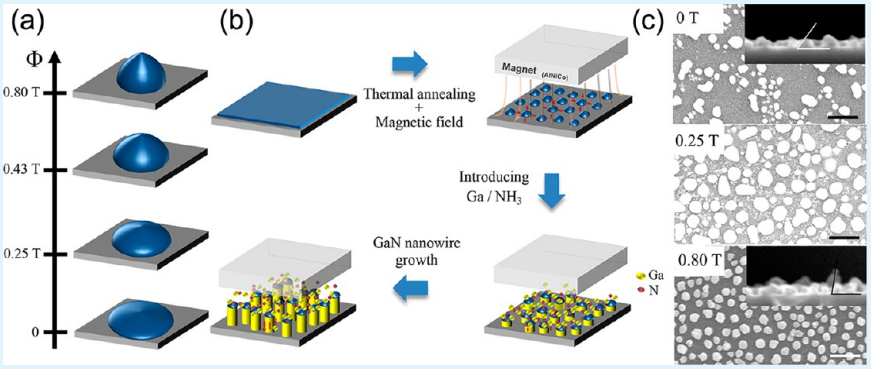

ABSTRACT: We report the growth of GaN nanowires at a low temperature of 750 °C and at atmospheric pressure in a conventional chemical vapor deposition (CVD) setup via the vapor−liquid−solid mechanism with remarkable control of directionality and growth behavior by using an in situ magnetic field. Under typical growth conditions, without any magnetic field, the nanowires are severely twisted and kinked, and exhibit a high density of planar stacking defects. With increasing in situ magnetic field strength, the microstructural defects are found to decrease progressively, and quasi-aligned nanowires are produced. At an applied magnetic field strength of 0.80 T, near-vertical aligned straight and several micrometers long nanowires of average diameter of ∼40 nm with defect-free microstructure are routinely produced. Photoluminescence measurements show that the relative intensity of the defect-related peaks in the visible region with respect to the near-band-edge emission continuously decrease with increase in the applied in situ magnetic field strength, ascribable to the magnetic field-assisted significant structural improvement of the wires. It is found out that the degree of agglomerative Ni droplet on Si is critically influenced by the surface tension driven by the magnetic force, which in turn determines the eventual properties of the nanowires.

KEYWORDS: *GaN, nanowires, chemical vapor deposition, magnetic field, growth mechanism*

INTRODUCTION

One-dimensional (1D) semiconducting nanowires have been extensively studied as critical solutions for next generation electronic and optoelectronic devices because of the extraordinary performance of their size/geometry-dependent properties.[1−4] There have been a lot of examples of promising nanowire-based devices actually showing better performance than the corresponding thin films or bulk materials. Nevertheless, the realization of the full potential of these nanowires has been limited by the difficulty in obtaining high quality growth, specific orientation, and spatial manipulation of nanowires into complex but ordered nanoscale architectures. Even until now, considerable progress has been made in achieving controllable nanowires by using different growth techniques with a concern for the accompanying processing cost.[5−8] The bottom-up approaches for growing nanowires, including solution growth, chemical vapor deposition (CVD) via the vapor−liquid−solid (VLS) mechanism, and electrochemical deposition using nanoporous templates, are considered more competitive because of their general lower cost compared to the top-down approaches typically employing lithography techniques.[5−8] However, the bottom-up approaches generate the random alignment of nanowires with kinks and twists, which must be avoided for actual applications. The post-growth assembly using the inferior nanowires for target configurations has shown the limitation in realizing highly integrated nanodevices.[9−11] The use of an external magnetic field for the controllable assembly of nanowires presents a noncontact and "easy-to-implement" way that can be successful on a large scale.[12−17] A few research groups have

Received: July 28, 2013
Accepted: October 11, 2013
Published: October 11, 2013

 © 2013 American Chemical Society

demonstrated magnetic manipulation of certain nanostructures including carbon nanotubes, metallic ferromagnetic nanowires, Ni-capped ZnO nanowires, and nonmagnetic metallic nanorods in a ferro-fluid.[12−17] In most of the above examples, however, the magnetic field has been used for the post-growth alignment of the nanostructures but not during the formation/growth stage. In the context of the popular VLS mechanism in the CVD process, the in situ application of an external magnetic field can be of great interest since the shape and the growth direction of nanowires can be determined by the morphology of solid−liquid interface and surface tension of the liquid alloy droplets during growth under the magnetic field.

In this work, in situ growth behavior and controllability of the alignment of GaN nanowires using an external magnetic field through the VLS mechanism in a CVD setup have been investigated. In a past few decades, GaN, a wide and direct band gap semiconductor, has been widely studied for applications in full color displays, blue LED, high electron mobility devices, and so forth.[18,19] Although many reports on CVD-grown GaN nanowires are available, the present work contrasts with them in that (1) an attempt has been made to grow nanowires using a ferromagnetic catalyst under the influence of a variable magnetic field strength and (2) near-ambient working pressure has been employed in the CVD chamber that may simplify the experimental procedure with viable cost advantages.

EXPERIMENTAL SECTION

Prior to the growth of GaN nanowires, a 10 nm-thick nickel layer was deposited as a catalyst on a Si (100) substrate by DC magnetron sputtering at a working pressure of 15 mtorr and a DC power of 100 W. Ar gas was introduced at a flow rate of 30 SCCM during the deposition. The optimum thickness of 10 nm of the Ni catalyst layer was determined by confirming the growth performance and quality of subsequent GaN nanowires in the evaluated thickness range of 5 to 100 nm.

A thermal CVD system was used to grow GaN nanowires. Trimethylgallium (TMG) as a source of Ga was vaporized at a fixed temperature of 750 °C under the gas flow of NH_3 and H_2 in a quartz tube having a diameter of 30 mm where the Ni-deposited Si substrate was positioned in the center of the tube. The deposition was performed for 1 h in atmospheric pressure. An AlNiCo magnet bar having a diameter of ∼12 mm was placed onto the top of the substrate prior to the deposition. The magnet is known to possess a Curie temperature of 850 °C,[20] which is suitable for the high temperature CVD processing. The magnetic field strength was controlled by varying the distance between the magnet and the substrate to ultimately have three different magnetic field strengths of ∼0.25, 0.43, and 0.80 T, as measured by a Gauss meter at room temperature. To understand the potential degradation of the magnetic field at elevated temperatures, the magnetic field of the magnet quenched from 750 °C was measured at room temperature. There was a decrease of about 14% in the field strength. Each time, a new magnet was used.

Surface morphology and the degree of alignment of nanowires were observed by high resolution field emission scanning electron microscopy (FESEM: JSM-6300, JEOL). Raman spectra were measured by a LabRam HR system (Hitachi) using a 514.5 nm Ar laser. Optical properties were investigated at room temperature by photoluminescence (PL) measurement using a 325 nm He−Cd laser. High-resolution transmission electron microscopy (HRTEM, Philips CM200FEG) was used to confirm the crystallinity and orientation of nanowires.

RESULTS AND DISCUSSION

Microstructural characteristics of GaN nanowires grown on the Ni-deposited Si substrate at 750 °C for 1 h under different magnetic field strengths (Φ) of 0, 0.25, 0.43, or 0.8 T were observed. Although it is known that a higher temperature is beneficial in producing good quality GaN,[21] a lower temperature is always desired to reduce the thermal cost and experimental complexity. Note that in the present case the processing temperature is well below the Curie temperature of the AlCoNi magnet that is commercially available as having the highest Curie temperature of 850 °C.[20] The influence of the magnetic field is very apparent from the increasing tendency of vertical alignments of the GaN nanowires, which are parallel to the direction of the magnetic field. The tangled nanowires with random growth directions, which were distinctively observed in the case of no magnetic field, tended to disappear gradually with increasing magnetic field. Depending on the level of magnetic field, the dimensions of the as-grown nanowires are ∼40−100 nm in diameter and ∼2-3 μm in length. The variation of the average diameter of the nanowires with the magnetic field strength is shown in Figure 1a. The diameter tended to decrease gradually to the level of ∼40 nm with increasing magnetic field up to 0.8 T.

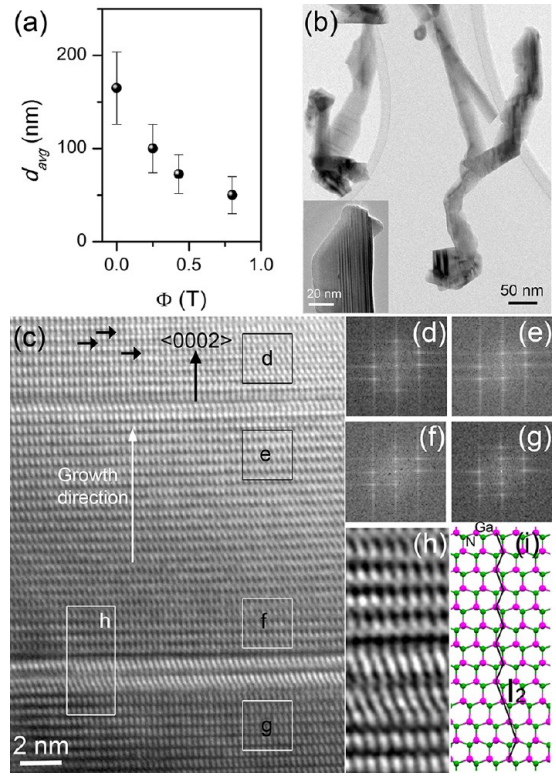

Figure 1. (a) Variation in average diameter of the GaN nanowires as a function of applied magnetic field strength Φ; (b) low magnification TEM images of the GaN nanowires grown without any magnetic field. Inset shows a HRTEM image of the top portion of a nanowire. The visible striations running along the growth direction of the wire correspond to planar stacking faults; (c) HRTEM image of one of the nanowires shown in panel (b) indicating the presence of a high density of stacking faults. The horizontal arrows show some examples of such faults. The growth direction was determined to be ⟨0002⟩ of the wurtzite phase; (d)−(g) FFT reciprocal lattice spots of corresponding selected regions marked in panel (c). The identical patterns indicate that the growth direction remains the same despite numerous stacking faults; (h) Fourier filtered image of a region in (c) that contains two I_2 type stacking faults in the wurtzite GaN nanowire; (i) Model of a single I_2 type stacking fault shown in panel (h).

dx.doi.org/10.1021/am403085y | ACS Appl. Mater. Interfaces 2014, 6, 116−121

Figure 1b shows an example of transmission electron microscopy (TEM) image of a few nanowires grown without any magnetic field ($\Phi = 0$). Most of the nanowires had arbitrary shapes characterized by multiple kinks and twists. A close inspection of the nanowires revealed a large density of crystallographic defects and complex growth patterns. As an example, the inset to Figure 1b shows a high resolution TEM (HRTEM) image of the top portion of a nanowire shown in Figure 1b. The nanowire was severely tapered, and clear visible striations, which correspond to planar stacking faults, were observed along the growth direction. A droplet, which is assumed to be the catalytic tip, was found to be displaced to the side of the nanowire. The tapering of the nanowire and the formation of a side-way tip indicate the onset of kink and/or change in growth direction of the nanowire. Figure 1c shows the HRTEM image of one of the GaN nanowires from Figure 1b indicating the presence of a high density of stacking faults. The horizontal arrows show some examples of such faults. Based on the analysis of the lattice fringes, the growth direction was determined to be ⟨0002⟩ of the wurtzite phase. The investigation of the growth pattern of the nanowire was carried out using the FFT-based analysis. The FFT reciprocal lattice spots of corresponding selected regions marked in Figure 1c are shown in Figures 1d–g. The identical FFT patterns indicate that the growth direction remained the same despite numerous stacking faults. The stacking faults are the planar defects arising because of a change in the stacking sequence of the atomic planes in the system and have been frequently reported for the wurtzite nanowires and nanobelts. Depending upon the number of layers extracted or inserted, the wurtzite structure can have three possible types of stacking faults, I_1 (one layer extracted), I_2 (two layers extracted), and E (one layer inserted).[23,24] Typically, in comparison to the ABABAB stacking sequence parallel to the (0001) plane in the wurtzite structure, the atomic planes are arranged in a different sequence as ...ABABCACABAB... in the I_1 an, I_2 type faults. A region containing two I_2 type stacking faults in the wurtzite GaN nanowire is marked (in a rectangle as "h") in Figure 1c, and the corresponding Fourier filtered image is presented in Figure 1h for clarity. The structural model of a single I_2 stacking fault is presented in Figure 1i.

The presence of an external magnetic field yielded quasi-aligned GaN nanowires with wurtzite crystal structure and with growth direction parallel to the c-direction ⟨0002⟩. More importantly, the stacking faults observed for the nanowires grown without any magnetic field strength were progressively removed with increasing magnetic field. As examples, micrographs and detailed lattice images for the GaN nanowires grown at Φ = 0.8 T are shown in Figures 2a–d. Several micrometer long nanowires free of kinks and twists have been successfully obtained (Figure 2a). The average diameter of the nanowires is about 40 nm, which is comparable to that of the nanowires grown using commercially available colloidal Au nanocrystals as a catalyst. The electron micrographs clearly show that the nanowires are smooth, straight, and more importantly, uniform in diameter along the entire length without any tapering. Furthermore, the HRTEM analysis revealed that there was no amorphous sheath on the surfaces of the nanowires. The higher growth rate and control of diameter uniformity by an alloy droplet at the tip (clearly observed in Figure 2b) are regarded as distinct features of the tip-led VLS/vapor–solid–solid (VSS) growth mechanism.[7,25,26] The EDS analysis of the tip and body of the

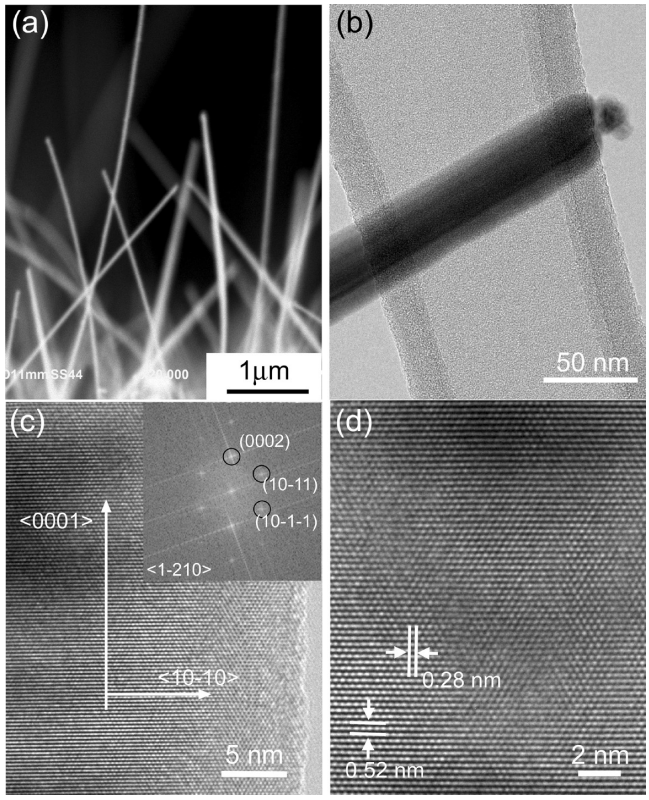

Figure 2. (a) Cross-sectional FESEM images of GaN nanowires grown at 750 °C under atmospheric pressure in the presence of magnetic field of 0.8 T. (b) HRTEM image of a GaN nanowire shows the presence of a near-spherical droplet at the tip, indicating the VLS growth mechanism. (c) HRTEM image at a larger magnification of the specimen in (b). The inset is an indexed FFT of the HRTEM image and the zone axis is ⟨1–210⟩. (d) shows the lattice images wherein the marked spacings of 0.52 and 0.28 nm correspond respectively to (0002) and (10–10) planes.

nanowires revealed that the tip consisted of Ga and Ni while no trace of Ni could be found on the body of the nanowires. This, along with the near-spherical shape of the droplet at the tip (indicating molten catalyst in liquid state), suggests the prevalent VLS growth mechanism in the present study. The clear lattice fringes indicate high crystallinity of the nanowires, which is also supported by the presence of distinct spot patterns in the corresponding FFT image (inset to Figure 2c). Analysis of the lattice images (Figures 2c and 2d) showed the interplanar spacing of ∼0.52 nm, and the FFT revealed preferential growth of the nanowires along the ⟨0002⟩ direction, which is expected on the basis of lower surface energy planes in the wurtzite structure.

On the basis of the HRTEM results presented above, the growth behavior is analyzed in conjunction with the VLS mechanism, wherein it has been suggested that a liquid metal cluster provides favorable sites for absorption of the gaseous reactants and subsequent nucleation/growth of the nanowires. A schematic illustration of shape evolution of the Ni islands and the growth of the GaN nanowires is presented in Figures 3a and b. At the reaction temperature, the gaseous Ga and N are absorbed in the Ni catalyst to form a probable Ni–Ga–N alloy that maintains a liquid phase as the catalytic reaction proceeds. When the concentration of Ga–N attains a saturation point in the Ni–Ga–N droplet because of steady flow of Ga and N, the Ga and N constituents diffused through the liquid phase to the

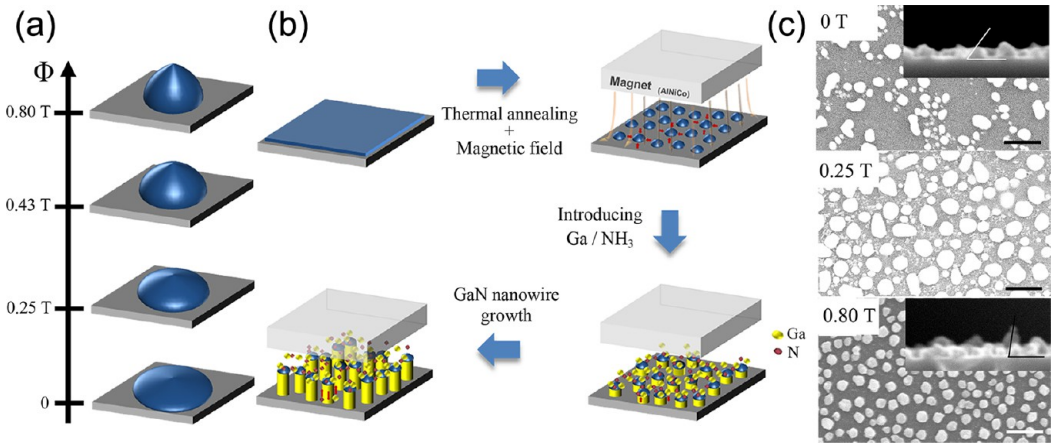

Figure 3. Schematic representation of (a) the size and shape evolution of the Ni dots influenced by the magnetic field strength and (b) the growth of quasi-aligned GaN nanowires at 0.80 T. The growth of the wires follows the VLS mechanism; (c) SEM images showing that at 750 °C the continuous Ni catalyst layer has dewet and agglomerated into well-separated dots, the size and distribution of Ni dots being strongly affected by the magnetic field strength of 0, 0.25, and 0.80 T. The scale bar in each figure corresponds to 1 μm. Insets in panel (c) are the cross-sectional view showing the wetting angle at interface.

bottom of the droplet start to precipitate out as GaN at the initial stage of growth. This is manifested as nanowires terminated with a droplet of alloy of catalytic metal and Ga, as observed in our case (Figure 2b). Furthermore, we found that in the absence of the Ni layer, there was no growth of nanowires either entangled or quasi-aligned, which confirms the catalyst supported VLS growth process.

In addition, the influence of the Ni catalyst is believed to be very critical in determining the growth quality of the GaN nanowires. It is well-known how various potential catalysts act during the VLS process of GaN nanowires[22,25,26] even though the effect of the external magnetic field has not been reported so far. As shown in Figure 3c, the average size/shape and distribution of the Ni dots are strongly affected by the magnetic field. For example, a very uniform distribution of Ni dots with nearly equalized size in the range of ∼40−70 nm was clearly found above the magnetic field of 0.43 T. It is worth recalling that the status of initially-formed Ni dots determines the distribution and size of the subsequent GaN nanowires in the VLS process.

Surface tension would critically play in defining the final size of Ni dots when Ni starts to move initially for consolidation into droplets at the elevated temperature of 750 °C under the magnetic field. Since the magnetic field itself is uniformly distributed, the influencing force on moving Ni droplets for consolidation should also be uniform. Probably, the contact angle is one of the parameters indicating the effectiveness of surface tension-driven consolidation.[27] The calculation of the contact angle using two selected examples of 0 and 0.8 T samples, as indicated in the insets of Figure 3c, showed the value of ∼48 and ∼80°, respectively. It confirms that the magnetic field tended to pull out the Ni catalyst towards the magnet and resulted in a higher contact angle. There is no comparative report in dealing with the interaction between catalyst and magnetic field except for the case of carbon nanofibers grown with iron catalyst under a magnetic field.[28] Although the report proposed that the magnetic field influenced the growth directionality of the carbon nanofibers, there was no systematic evidence of relating the influence of magnetic field to the catalytic behavior during the growth. Nevertheless, supported by the above observations, it is believed that application of the higher magnetic field resulted in the uniform distribution of size and shape of the initial Ni catalyst dots that favored growth of nanowires of better crystalline quality.

Figure 4 exhibits the Raman spectra of GaN nanowires prepared under different magnetic field strengths in the range

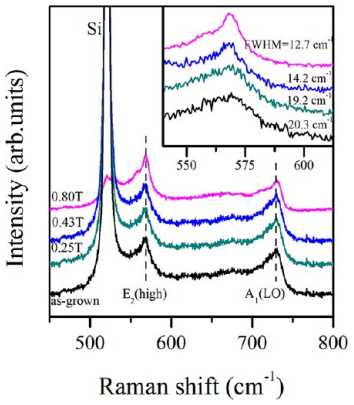

Figure 4. Raman spectra of GaN nanowires magnet-assisted grown at various magnetic field strengths ranging from 0 to 0.80 T. The inset is a close up of the spectral region from 540 to 620 cm^{-1}. The FWHM of the E_2 (high) modes is also given.

of 450 to 800 cm^{-1}. As expected from the Raman reports for the GaN nanowires, the spectra are characterized with two strong Raman−active phonon bands near 568.2 cm^{-1} and 730 cm^{-1}, corresponding to the E_2 (high) and A_1 (LO) modes, respectively, thus confirming the wurtzite structure of GaN.[29−31] The vicinity of the E_2 (high) phonon peak of GaN nanowires is highlighted as inset in Figure 4. The E_2 (high) mode was observed at 570.1 cm^{-1} for the as-grown sample, 568.9 cm^{-1} at 0.25 T, 568.4 cm^{-1} at 0.43 T, and 567.0 cm^{-1} at 0.80 T. Compared to the reference peak of 569 cm^{-1} as reported for GaN,[29−31] all samples grown in the magnetic field correspond to a red-shift. The shift in peak position of the E_2 (high) mode is known to be related to the existence of stress in the nanowires.[29−31] The stress was evaluated by the simple relation of $\Delta\omega(E_2) = k\sigma$, where $\Delta\omega$ is the peak shift in

dx.doi.org/10.1021/am403085y | ACS Appl. Mater. Interfaces 2014, 6, 116−121

wavelength, σ is the biaxial stress, and k is the proportionality factor, typically in the range of $2.7 < k < 7.6$ for GaN.[25,26] Assuming the k value of 6.2 as reported for GaN nanowires,[29] the magnitude of stress induced by the magnetic field was estimated. The tensile stress incurred by the red-shift tended to increase from 0.02 to 0.27 GPa with increasing magnetic field strength, while the nanowires grown in no magnetic field demonstrated a compressive stress (blueshift) of ~0.17 GPa. Tensile stress may occur in the growing nanowires when a material is subject to the pulling force driven by a magnetic force through the Ni tips used here. On the other hand, compressive stress in nanowires has been more generally recognized as a result of the lattice contraction caused by the mismatch in thermal expansion between GaN nanowires and Si substrate.[31] In addition, the full width at half maximum (FWHM) of the E_2 (high) peaks was examined from the Lorentz-fitted Raman spectrum. The smaller FWHM values were observed with increasing magnetic strength, suggesting that the application of the magnetic field enhances the crystallinity of the nanowires. For instance, the values of ~20.3 and ~12.7 cm^{-1} were obtained at 0 and 0.80 T, respectively.

Room temperature photoluminescence (PL) spectra of the GaN nanowires grown at different magnetic field strength Φ are shown in Figure 5. Each sample showed three GaN-related

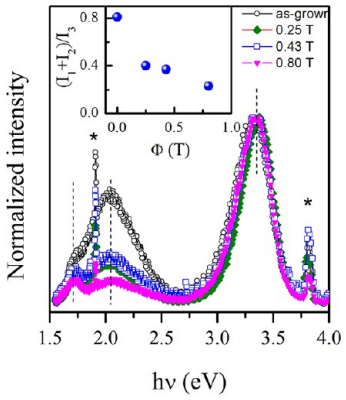

Figure 5. Room-temperature PL spectra of the GaN nanowires grown at different magnetic field strengths. Each spectrum has been normalized with respect to the corresponding NBE peak at 3.35 eV. The peaks marked by asterisk (*) are associated with the laser excitation source. The vertical dotted lines show three clear peaks I_1, I_2, and I_3 (with increasing energy). Inset shows the variation in intensity ratio of visible to NBE PL peak $(I_1+I_2)/I_3$ as a function of magnetic field strength Φ.

distinct peaks occurring at about 1.71, 2.05, and 3.35 eV (labeled as peak 1, 2, and 3, respectively) and two sharp peaks at ~1.9 and 3.8 eV (marked by asterisk in the figure) due to the laser excitation source. The peaks in the visible region (peak 1 and 2) are suggested to be associated with surface disorder, interior defects of nanowires, and donor−acceptor pair transitions from defects in nanowires,[32] while the peak 3 is more closely related to the fundamental absorption process. The near-band-edge (NBE) peak (peak 3) remained the same in intensity and FWHM irrespective of the magnetic field strength. However, the peak position for all samples showed slight red-shift in the range 20−60 meV compared with that of the perfect GaN film and bulk. This might be due to the change in band gap caused by stress in the nanowires.[33,34] On the other hand, the visible peaks 1 and 2 exhibited strong dependence on the magnetic field strength. As seen from the inset of Figure 5 that depicts the variation in the intensity ratio of visible to NBE PL peaks $(I_1 + I_2)/I_3$ as a function of magnetic field strength Φ, the relative intensity of the defect-related visible peaks continuously decreased with increase in the magnetic field strength suggesting the structural improvement of the wires with increase in magnetic field strength. This behavior is agreement with the results of the Raman studies that showed the continuous decrease of the FWHM of the E_2 (high) modes and the HRTEM characteristics of the related crystallinity in straight nanowires due to the magnetic effect during the growth stage.

CONCLUSIONS

For the first time we have reported growth of GaN nanowires at a relatively lower temperature of 750 °C and at atmospheric pressure by the CVD process via the VLS mechanism. It has been shown that remarkable control of directionality and growth behavior could be exercised by using an in situ magnetic field during the growth of the nanowires. The nanowires grown without any magnetic field were severely twisted and kinked, and exhibited a high density of planar stacking defects. With increase in the magnetic field, the defects were progressively removed, and quasi-alignment of the nanowires was obtained. For example, at an in situ applied magnetic field strength of 0.80 T, near-vertical aligned, straight, and several micrometers long nanowires of average diameter of ~40 nm with defect-free microstructure could be routinely produced. Raman and photoluminescence measurements revealed improved nanowire properties, clearly attributed to the magnetic field-assisted significant structural improvement of the wires. It was found that the degree of agglomeration of Ni droplets on Si was critically influenced by the surface tension driven by the magnetic force, which in turn determined the eventual properties of the nanowires. A growth model based on the magnetic field-assisted VLS process of nanowires has been presented.

AUTHOR INFORMATION

Corresponding Author

*E-mail: ycho@yonsei.ac.kr. Phone: 82-2-2123-5848.

Present Address

[⊥]School of Physics and Materials Science, Thapar University, Patiala 147004, India.

Author Contributions

[∥]These authors contributed equally.

Notes

The authors declare no competing financial interest.

ACKNOWLEDGMENTS

This work was supported by the National Research Foundation of Korea (NRF) grant funded by the Ministry of Education, Science and Technology. (No. 2011-0020285).

REFERENCES

(1) Xia, Y. N.; Yang, P. D.; Sun, Y. G.; Wu, Y. Y.; Mayers, B.; Gates, B.; Yin, Y. D.; Kim, F.; Yan, H. Q. *Adv. Mater.* **2003**, *15*, 353−389.
(2) Barth, S.; Hernandez-Ramirez, F.; Holmes, J. D. *Prog. Mater. Sci.* **2010**, *55*, 563−627.
(3) Sheng, X.; Wang, Z. L. *Nano Res.* **2011**, *4*, 1013−1098.

(4) Bachtold, A.; Hadley, P.; Nakanishi, T.; Dekker, C. *Science* **2001**, *294*, 1317−1319.
(5) Wagner, R. S.; Ellis, W. C. *Appl. Phys. Lett.* **1964**, *4*, 89−90.
(6) Duan, X.; Lieber, C. M. *Adv. Mater.* **2000**, *12*, 298−302.
(7) Purushothaman, V.; Ramakrishnan, V.; Jeganathan, K. *RSC Adv.* **2012**, *2*, 4802−4806.
(8) Li, H.; Chin, A. H.; Sunkara, M. K. *Adv. Mater.* **2006**, *18*, 216−220.
(9) Cook, B. G.; Varga, K. *Appl. Phys. Lett.* **2011**, *98*, 052104.
(10) Inoue, Y.; Hoshino, T.; Takeda, S.; Ishino, K.; Ishida, A.; Fujiyasu, H.; Kominami, H.; Mimura, H.; Nakanishi, Y.; Sakakibara, S. *Appl. Phys. Lett.* **2004**, *85*, 2340−2342.
(11) Jeong, M. C.; Lee, S. W.; Seo, J. M.; Myoung, J. M. *Nanotechnology* **2007**, *18*, 305701.
(12) Yuan, J.; Gao, H.; Schacher, F.; Xu, Y.; Richter, R.; Tremel, W.; Muller, A. H. E. *ACS Nano* **2009**, *3*, 1441−1450.
(13) Hangarter, C. M.; Myung, N. V. *Chem. Mater.* **2005**, *17*, 1320−1324.
(14) Tanase, M.; Bauer, L. A.; Hultgren, A.; Silevitch, D. M.; Sun, L.; Reich, D. H.; Searson, P. C.; Meyer, G. J. *Nano Lett.* **2001**, *1*, 155−158.
(15) Lee, S. W.; Jeong, M. C.; Myoung, J. M.; Chae, G. S.; Chung, I. J. *Appl. Phys. Lett.* **2007**, *90*, 133115.
(16) Bentley, A. K.; Trethewey, J. S.; Ellis, A. B.; Crone, W. C. *Nano Lett.* **2004**, *4*, 487−490.
(17) Chinchun, O.; Randall, M. E.; Benjamin, B. Y. *J. Appl. Phys.* **2008**, *103*, 07E910.
(18) Chen, L. C.; Chen, K. H.; Chen, C. C. Group III- and Group IV-nitride Nanorods and Nanowires. In *Nanowires and Nanobelts - Materials, Properties and Devices*; Wang, Z. L., Eds.; Kluwer Academic: Boston, 2003; Vol. *1*, pp 25−30.
(19) Chattopadhyay, S.; Ganguly, A.; Chen, K. H.; Chen, L. C. *Crit. Rev. Solid State Mater. Sci* **2009**, *34*, 224−279.
(20) Tsutsui, H.; Kinouchi, Y.; Sasaki, H.; Ushita, T. *J. Dent. Res.* **1979**, *58*, 1597−1606.
(21) Weng, X.; Burke, R. A.; Redwing, J. M. *Nanotechnology* **2009**, *20*, 085610.
(22) Kuykendall, T.; Pauzauskie, P. J.; Zhang, Y.; Goldberger, J.; Sirbuly, D.; Denlinger, J.; Yang, P. *Nat. Mater.* **2004**, *3*, 524−528.
(23) Potin, V.; Ruterana, P.; Nouet, G. *J. Phys.: Condens. Matter* **2000**, *12*, 10301−10306.
(24) Stampfl, C.; Van de Walle, C. G. *Phys. Rev. B: Condens. Matter Mater. Phys.* **1998**, *57*, R15052.
(25) Givargizov, E. I. *J. Cryst. Growth* **1975**, *31*, 20−30.
(26) Wu, Y.; Yang, P. *J. Am. Chem. Soc.* **2001**, *123*, 3165−3166.
(27) Gibbs, J. W. *The Scientific Papers of J. W. Gibbs*; Dover: New York, 1961; Vol. *1*.
(28) Sun, L. F.; Liu, Z. Q.; Ma, X. C.; Tang, D. S.; Zhou, W. Y.; Zou, X. P.; Li, Y. B.; Lin, J. Y.; Tan, K. L.; Xie, S. S. *Chem. Phys. Lett.* **2001**, *336*, 392−396.
(29) Lee, K. H.; Chen, I. G. *J. Electrochem. Soc.* **2009**, *156*, K59−K63.
(30) Orton, J. W.; Foxon, C. T. *Rep. Prog. Phys.* **1998**, *61*, 1−75.
(31) Kozawa, T.; Kachi, T.; Kano, H.; Nagase, H.; Koide, N.; Manabe, K. *J. Appl. Phys.* **1995**, *77*, 4389−4392.
(32) Reshchikov, M. A.; Morkoc, H. *J. Appl. Phys.* **2005**, *97*, 061301.
(33) Wang, Y. D.; Chua, S. J.; Tripathy, S.; Sander, M. S.; Chen, P.; Fonstad, C. G. *Appl. Phys. Lett.* **2005**, *86*, 071917.
(34) Zhang, X.; Liu, Z.; Wong, C.; Hark, S. *Solid State Commun.* **2006**, *139*, 387−390.